Int. J. Electrochem. Sci., 9 **(2014)** 4413 - 4428

International Journal of
ELECTROCHEMICAL
SCIENCE
www.electrochemsci.org

Corrosion Resistance of Electrodeposited Ni-Mo-W Coatings

Paulo N. S. Casciano[*], *Ramon L. Benevides, Pedro de Lima-Neto, Adriana N. Correia*

Departamento de Química Analítica e Físico-Química, Centro de Ciências, Universidade Federal do Ceará, Bloco 940, Campus do Pici,60440-900, Fortaleza-CE, Brazil
[*]E-mail: paulonaftali@ufc.br

Received: 4 April 2014 / *Accepted:* 7 May 2014 / *Published:* 19 May 2014

A comparative investigation was carried out with electrodeposited Ni-W and Ni-Mo-W coatings to evaluate the influence of Mo content on the corrosion resistance. Corrosion tests were carried out by potentiodynamic linear polarization, electrochemical impedance spectroscopy and open circuit monitory, in NaCl solution. Ni-W and Ni-Mo-W coatings were obtained by electrodeposition and Mo content in the layer increased with the molybdenum ion concentration in the electrolyte. Cracked and non-cracked coatings were obtained resulting in nanocrystalline or amorphous coatings. Finally, the addition of Mo improved the corrosion resistance of the Ni-W based coatings in neutral medium.

Keywords: Ni-W, Ni-Mo-W; Corrosion resistance; Electrochemical impedance spectroscopy; Potentiodynamic linear polarization.

1. INTRODUCTION

Spite its well-known high toxicity to aquatic environment and to human health, chromium is used in several industrial practices. One of the most used technological applications of this metal is the called hard chromium coating that is produced by electrodeposition from a plating solution containing Cr^{6+}. This coating continues been widely used due to its excellent properties such as high hardness, low coefficient of friction and good performance against corrosion and wear [1]. It is its poor environmental reputation, associated to its toxicity, which has led to a growing environmental appeal to restrict its use in industrial practice. Therefore, it is current the efforts to find environmental friendly coatings that effectively come to become alternatives to Cr coatings [1]. As possible alternative, electrodeposited tungsten coating could be the most promising candidate to replace hard chromium coating, since W is of the Cr group in the periodic table and it would be expected that the electrodeposit of this metal present similar properties than that presented by the hard chromium coating. Additionally, tungsten alloys may have similar hardness values the chromium alloys or even

higher [2, 3] and it is resistant to high temperatures due to its higher melt point (t = 3680 °C) [3], while the Cr melt point is 2130 °C [4].

Unfortunately, this metal cannot be electrodeposited alone from aqueous solution and the metallic W only can be obtained from the co-electrodeposition with Fe, Co and Ni ions and in the presence of complexing agents [5-9]. Among them, nickel is certainly the best choice because it has good corrosion resistance, good ductility, relatively high hardness and good electrical conductivity.

The environmental motivation for the interest in the electroposited Ni-W coatings is that the Ni-W plating solutions are formulated using tungstate as the W source, and this ion is known to present mildly toxicity [4, 10]. The solutions for obtaining the electrodeposited Ni-W coatings are usually formulated at alkaline pH using citrate and the ammonium as complexing agent. Younes and Gileadi [8] studied the electrodeposition of Ni-W coatings from aqueous solution containing citrate and ammonia and they evaluated the bath composition, the current density and rotation rate and found that the citrate and ammonia concentrations were outstanding in the faradaic efficiency and tungsten content. For bath containing excess of ammonia, the tungsten content in the coating was limited, while the faradaic efficiency increased. On the other hand, the increase in citrate concentration led to a decrease in the faradaic efficiency. In addition, Alimadadi *et al*. [9] studied the corrosion properties of Ni-W coatings containing high tungsten content. They showed that the tungsten content in the electrodeposited coating increased with the tungstate concentration in the plating solution, resulting in increase of corrosion resistance.

Furthermore, it is known that functional properties of electrodeposited coatings depend on their composition. Therefore, the addition of a third metal can improve the properties of a binary Ni-W coating, such corrosion resistance and microhardness. A potential candidate to be added to Ni-W coatings is the Mo, another member of the Cr group of the periodic table, since the Mo-based plating solutions are formulated with the ion molybdate (MoO_4^{2-}) and this ion is environmental acceptable because of it is low toxicity [11]. Thus, a systematic investigation of the electrodeposition of the ternary Ni-Mo-W coatings was carried out aiming to evaluate the influence of Mo on the corrosion resistance of Ni-W based coatings and a comparative study with the binary electrodeposited Ni-W coating is also presented.

2. EXPERIMENTAL PART

2.1. Electrodeposition

The solutions were prepared form analytical grade purity chemicals dissolved in purified water by a Millipore Milli-Q system. Ni-Mo-W coatings were electrodeposited from electrolyte containing 0.15 mol dm^{-3} H_3BO_3, 0.056 mol dm^{-3} $(NH_4)_2SO_4$, 10^{-4} mol dm^{-3} $CH_3(CH_2)_{10}CH_2OSO_3Na$, 0.65 mol dm^{-3} $Na_3C_6H_5O_7.2H_2O$, 0.2 mol dm^{-3} $NiSO_4.2H_2O$, 0.3 mol dm^{-3} $Na_2WO_4.2H_2O$ and 0-0.1 mol dm^{-3} $Na_2MoO_4.2H_2O$. The plating solution for the electrodeposition of the Ni-W coating was formulated using all compounds in the same concentration, but without the addition of $Na_2MoO_4.2H_2O$. The pH of the electrolytic solutions was adjusted to 10 by adding concentrated ammonia. The coatings were

electrodeposited on disc-shaped Cu substrate embedded in epoxy resin with an exposed geometric area of approximately 2 cm^2. The electrodepositions were performed in a single-compartment Pyrex® glass cell with a Teflon® cover containing holes to fix the Cu cathode and the platinum plate anode. Prior to the alloy plating, the Cu surface were polished with 100, 400 and 600 SiC emery paper, degreased in a 10 % NaOH solution, rinsed in distilled water, etched in 10 % HCl solution and finally rinsed again in distilled water. The coatings were electrodeposited under galvanostatic control at 60 mA cm^{-2}, at 26 ^oC and with a total charge of 250 C.

2.2. Physical and chemical characterization

The surface and cross-section morphologies of the deposited coatings were analyzed using a Vega XMU Tecsan USA scanning electron microscope (SEM). The SEM cross section allowed the determination of the coating thickness. The coatings compositions were analyzed by an energy dispersive X-ray (EDX) apparatus attached to the SEM. The EDX analyses were carried out on the surface and on a cross-section of the coatings, and the sample composition were uniform over the two analyzed regions.

The coating crystal phase structure was analyzed by X-ray Diffraction (XRD) using a DMAXB Rigaku diffractometer with radiation of the Cu ($k\alpha$ = 1.54056 Å) at 40 kV and 25 mA and incident angle of 3^o.

2.3. Electrochemical corrosion tests

The electrochemical experiments were performed at room temperature (26 °C) and using a conventional electrochemical cell for three electrodes. The Cu/Ni-W and Cu/Ni-Mo-W were the working electrodes, Ag/AgCl/Cl^-(saturated) electrode was the reference electrode and a foil Pt (2 cm^2) was the counter electrode. Potentiodynamic linear polarization (PLP) curves were obtained at 1 mV s^{-1}. Electrochemical impedance spectroscopy (EIS) diagrams were obtained in the frequency range of 40 kHz to 6 mHz with a sinusoidal amplitude of 10 mV and at open circuit potential. The measurements of PLP and EIE were carried out in 0.1 mol dm^{-3} NaCl aqueous solution.

The local pH measurements were employed to monitor pH at the electrode/electrolyte interface. It differs from the bulk solution, during the conversion process, in consequence of reactions producing or depleting H^+ ions. The experimental setup used in this work was similar to the one proposed by Calderón *et al*. [12]. The local pH measurements were accomplished with a flat pH electrode (HI1413B from Hanna Instruments) fixed in the electrochemical cell and connected to a pH meter B474 (Micronal), which monitored the changes on pH just after the cell was filled with the electrolytic solution. The working electrode was positioned in the bottom of the cell and their surfaces were close to the pH electrode. At these conditions, the pH local experiments were performed together with PLP in 0.1 mol dm^{-3} NaCl solution with a scan with a scan rate of 1 mV s^{-1}. Figure 1 shows an illustration of the assembled electrochemical cell for measuring the local pH.

An AUTOLAB PGSTAT 30 potentiostat/galvanostat, linked to a PC computer and controlled by GPES 4.9 and Nova 1.10 software, was used for the acquisition of the electrochemical data.

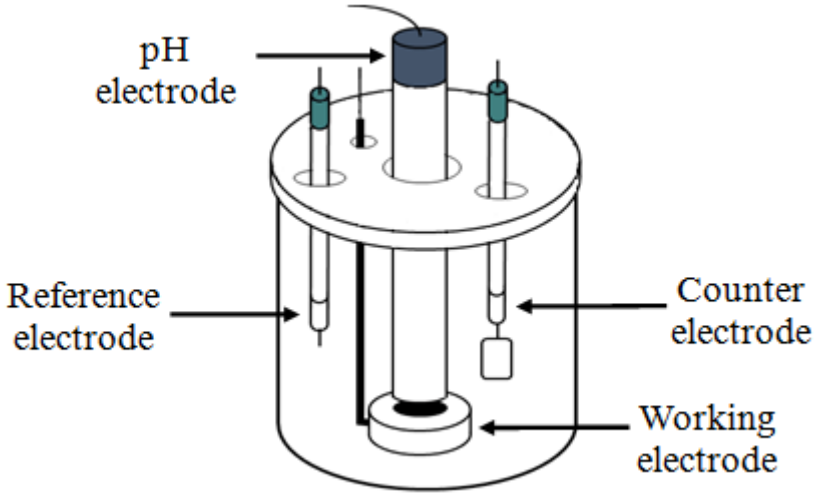

Figure 1. Drawing illustrating the electrochemical cell used for the local pH measurements.

3. RESULTS AND DISCUSSION

3.1. EDX analyses and current efficiency

Figure 2a shows the EDX profiles indicating the presence of W and Mo in the Ni-W or Ni-MoW coatings. Figure 2b allows analysing the influence of the MoO_4^{2-} concentration in the plating solution on the Mo and W contents in the layer. This figure shows that, in the range of 0.01 mol dm^{-3} to 0.08 mol dm^{-3}, an approximately linear relationship was observed between the MoO_4^{2-} concentration and the Mo content in the layer, which varied between 5 at% to 21 at%. For higher MoO_4^{2-} concentration, the Mo content in the layer slightly decreases for 19 at%. Without MoO_4^{2-} in the plating solution, the binary Ni-W electrodeposited coating contains about 4 at% of W. With the addition of 0.01 mol dm^{-3} MoO_4^{2-} in the plating solution, the W content in the Ni-Mo-W layer was about 8 at%. For the concentrations of the MoO_4^{2-} of 0.025 mol dm^{-3} and 0.05 mol dm^{-3}, the W content in the electrodeposited layer was approximately constant about 4 at%, slightly increasing for 5 and 6 at% for the MoO_4^{2-} concentrations of 0.075 and 0.1 mol dm^{-3}, respectively. Therefore, the W content in the layer was less influenced by the MoO_4^{2-} concentration in the electrodeposition bath than the Mo content.

SEM cross section analysis allowed the experimental determination of the thickness of the electrodeposited coatings, which was also included in Figure 2b. It can be observed that the experimental thickness decreases with MoO_4^{2-} concentration in the plating solution. This behaviour was

explained as being due to an increase in adsorbed hydrogen on the electrode surface during the electrodeposition as a consequence of the MoO_4^{2-} concentration in the plating solution [13].

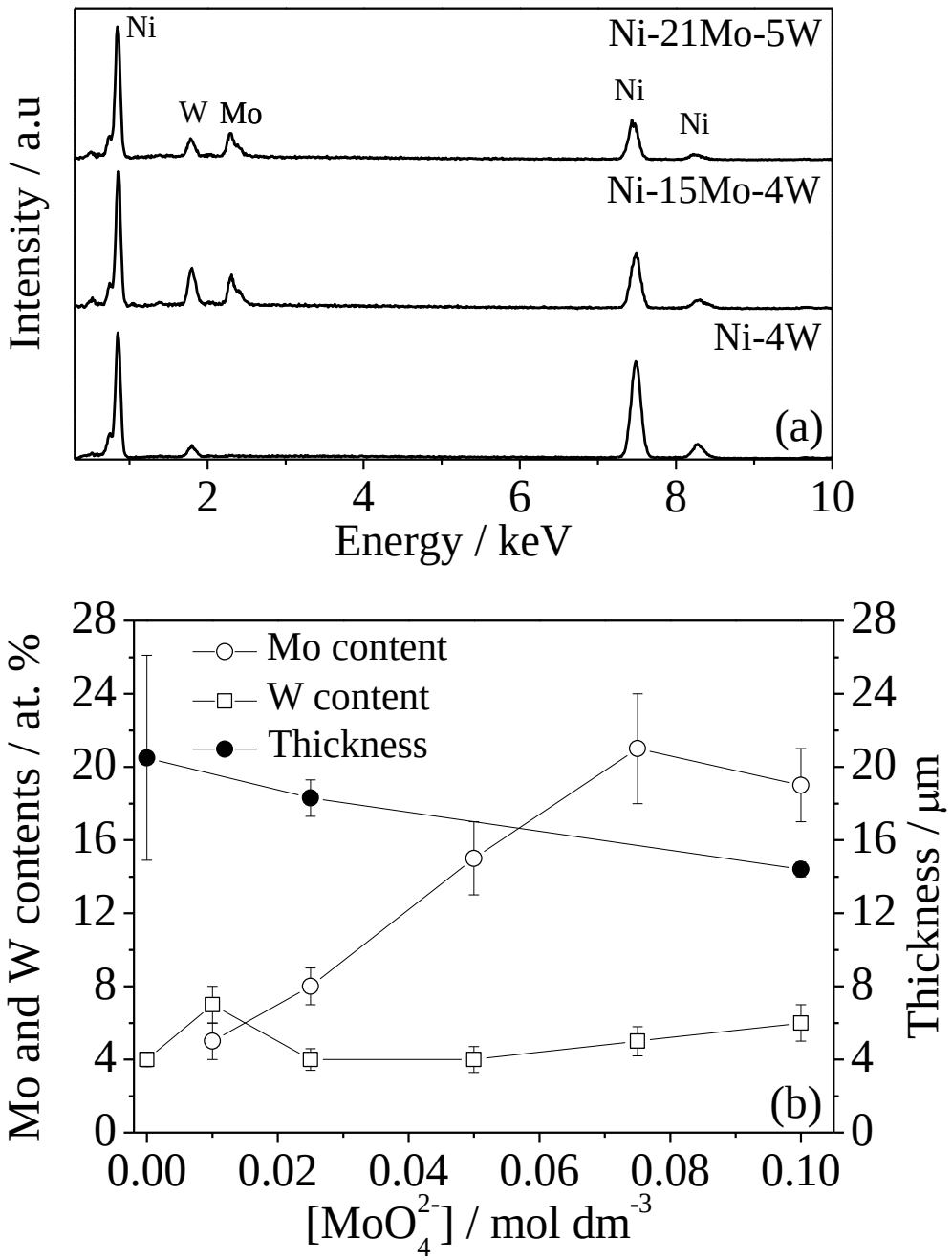

Figure 2. (a) EDX profiles for Ni-4W, Ni-15Mo-4W and Ni-21Mo-5W coatings; (b) Influence of the MoO_4^{2-} ion concentration in the plating solution on Mo and W contents in the electrodeposited Ni-Mo-W coatings and on the thickness of the electrodeposition process.

Selected SEM images of the surface morphology of the electrodeposited Ni-Mo-W coatings are displayed in Figure 3. The SEM images show that the Ni-Mo-W surfaces became smoother with increase the Mo content in the layer and that nuclei are present on the surface. The presence of nuclei

is explained as consequence of the growth of secondary nuclei on top of the layer that were formed in the primary nucleation phase. Furthermore, cracked ternary coatings were obtained with low Mo content in the electrodeposited layer, such as Ni-5Mo-7W (Fig. 3b) and Ni-8Mo-4W (Fig. 3c), while for higher Mo content the electrodeposited coatings were not cracked.

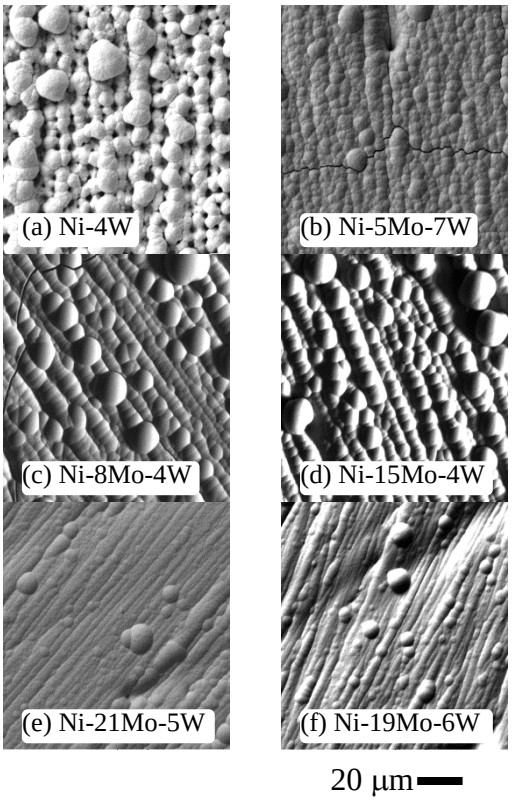

Figure 3. Surface SEM images of coatings obtained at 60 mA cm^{-2} and 0.15 mol dm^{-3} H_3BO_3 + 0.056 mol dm^{-3} $(NH_4)_2SO_4$ + 10^{-4} mol dm^{-3} $CH_3(CH_2)_{10}CH_2OSO_3Na$ + 0.65 mol dm^{-3} $Na_3Cit.2H_2O$ + 0.2 mol dm^{-3} $NiSO_4.2H_2O$ + 0.3 mol dm^{-3} $Na_2WO_4.2H_2O$ + x mol dm^{-3} $Na_2MoO_4.2H_2O$ solution at pH 10. (a) x=0, (b) x=0.01, (c) x=0.025, (d) x=0.05, (e) x=0.075, (f) x=0.1.

Unfortunately, there is not a clear explanation for the appearance of the cracks. Lammel *et al*. [14] and Eliaz *et al*. [15] claimed that the cracks often result from high residual stress or hydrogen embrittlement during electrodeposition. The size and number of cracks depended of the current density applied during electrodeposition, whereas Mizushima *et al*. [16] argued that the difference in thermal contraction between Cu and coating after deposition also led to a compressive stress in the layer.

The X-ray diffractograms of some coatings are shown in Figure 4. Initially, the peaks observed at 2θ angles centred at 43.5^o and at 50.5^o were related to the cupper substrate. For the binary Ni-W coating, two well characteristic peaks related to the nickel can be observed in the diffractograms at 2θ angles centred at 44.7^o and at 52^o. This result indicated that the binary electrodeposited coating was crystalline. This is in close agreement with Wang *et al*. [17] that electrodeposited Ni-W coatings from citrate-ammonia electrolyte. They showed that coatings with low W content were crystalline and it became amorphous by increasing the percentage of tungsten.

Two broad peaks were observed in the diffractogram of the Ni-8Mo-4W coating with 2θ angles equal to 44.7° and 53.4°, whereas for Ni-19Mo-6W the broad peak at 53.4° was not observed. The absence of characteristics peak related to Mo and W in these diffractograms was associated to the dissolution of Mo and W atoms in Ni, leading to a lattice expansion of Ni because there was a difference in atom size between the constituents of the coatings [18]. Alimadadi *et al*. [9] proposed the formation of two types of structures in the Ni-W coatings: (i) single phase nanostructure and (ii) two phase nanostructure in which a second Ni-W amorphous phase or even amorphous-disordered mixture separates the Ni nanoparticles. Therefore, the broad peaks observed in the diffractograms of the ternary coatings can be related to nanocrystalline or amorphous structure.

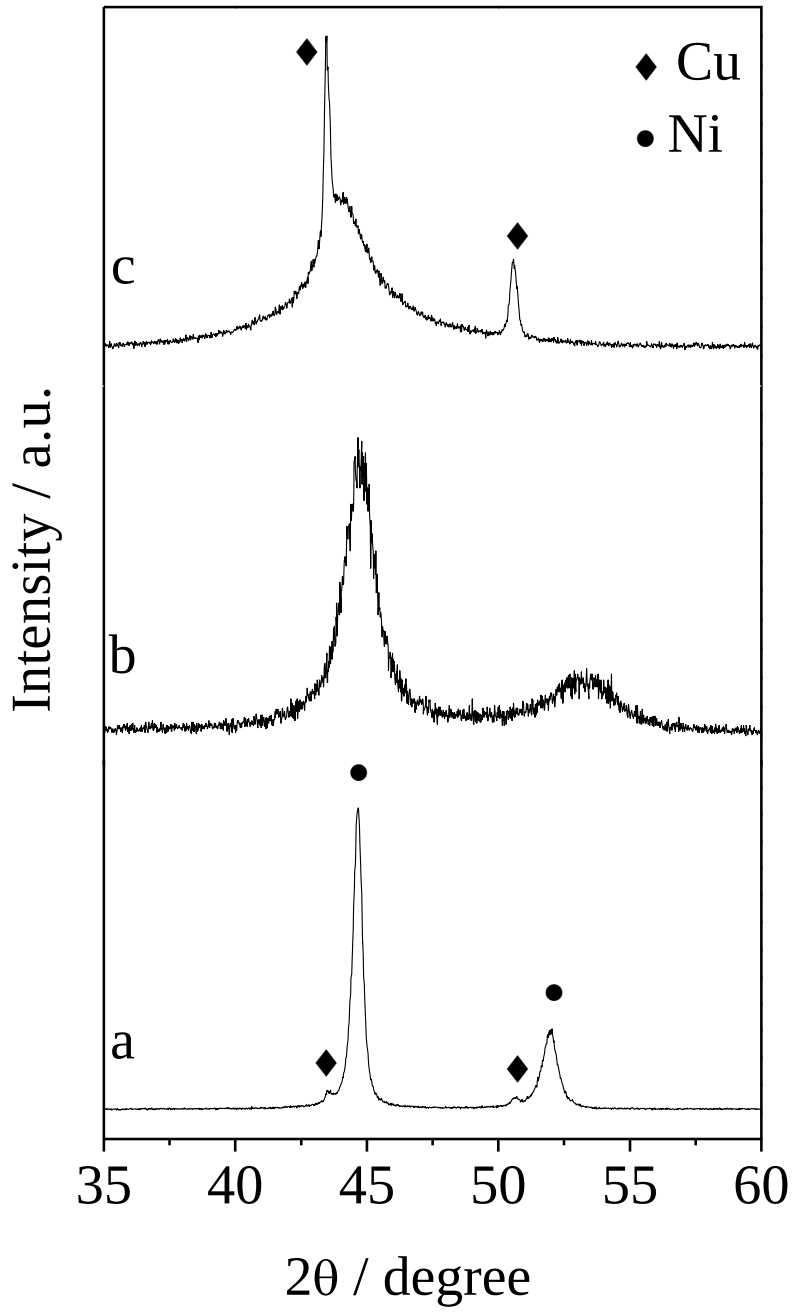

Figure 4. X-ray diffractograms for the as-electrodeposited obtained at 60 mA cm^{-2}: Ni-4W coating (a); Ni-8Mo-4W coating (b); and Ni-19Mo-6W coating (c).

3.2. Electrochemical corrosion tests

Non-cracked coatings were selected to electrochemical corrosion studies. The potentiodynamic polarization curves obtained in 0.1 mol dm^{-3} NaCl solution are shown in Figure 5.

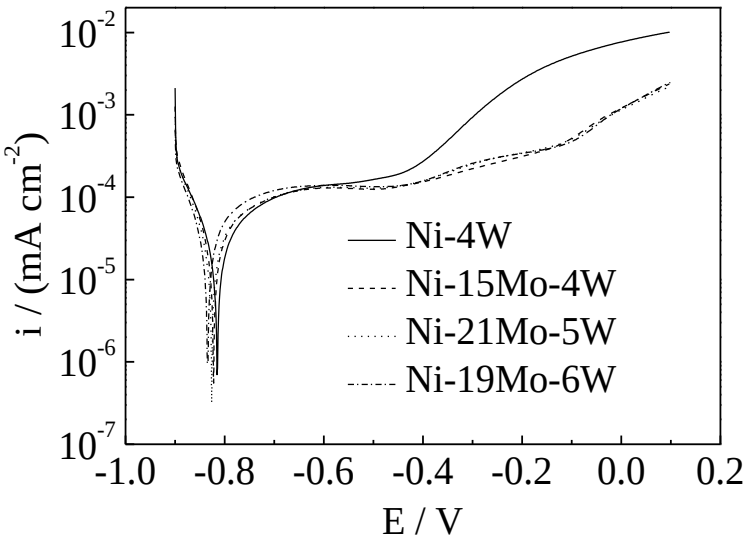

Figure 5. Potentiodynamic polarization curves obtained in 0.1 mol dm^{-3} NaCl solution at 1 mV s^{-1} for the electrodeposited Ni-W and Ni-Mo-W coatings obtained at 60 mA cm^{-2}.

This figure shows that the corrosion potential was independent of the coating composition. For the polarization curves obtained in NaCl solution (Fig. 5), an increase of the current density was observed between –0.8 V and –0.65 V, which was related to the active dissolution of the coatings. Between –0.65 V and –0.55 V, a short current density plateau was observed for the ternaries alloys while the current density for the Ni-W coating continued to grow at a slower rate. This was an indication that the dissolutions of Ni-W and Ni-Mo-W coatings in NaCl medium were kinetically limited in this potential range. For applied potential more positive potential than –0.55 V, current densities of the ternary alloys were lower than current density of the binary alloy and they rise with the applied potential, indicating generalized dissolution of the coatings. Therefore, these polarization curves showed that the Ni-Mo-W and Ni-W coatings corrode in chloride medium

The existence of the current densities plateau was associated with the formation of surface films oxides and hydroxides that can, initially, blocked the dissolution of the ternary coatings. The increase in current density that follows the current plateau was related to the breakdown of the surface film, leading to the dissolution of the coatings. Finally, the polarization curves obtained showed the positive effects of the Mo addition in Ni-W based coatings, that there was no difference in the electrochemical behaviour among the Ni-Mo-W coatings and that the better corrosion resistances were presented by the ternary Ni-Mo-W coatings.

Local pH was monitored during polarization curves obtained in 0.1 mol dm^{-3} NaCl medium in order to elucidate the electrochemical reactions that occur on the coating in neutral medium. The

Figure 6 shows these measurements for the electrodeposited Ni-4W and Ni-15Mo-4W in 0.1 mol dm^{-3} NaCl. The Pourbaix potential-pH diagrams [19] for Ni, Mo and W were used in order to associate the pH variation with possible chemical reactions that occur on Ni-4W and Ni-15Mo-4W surfaces.

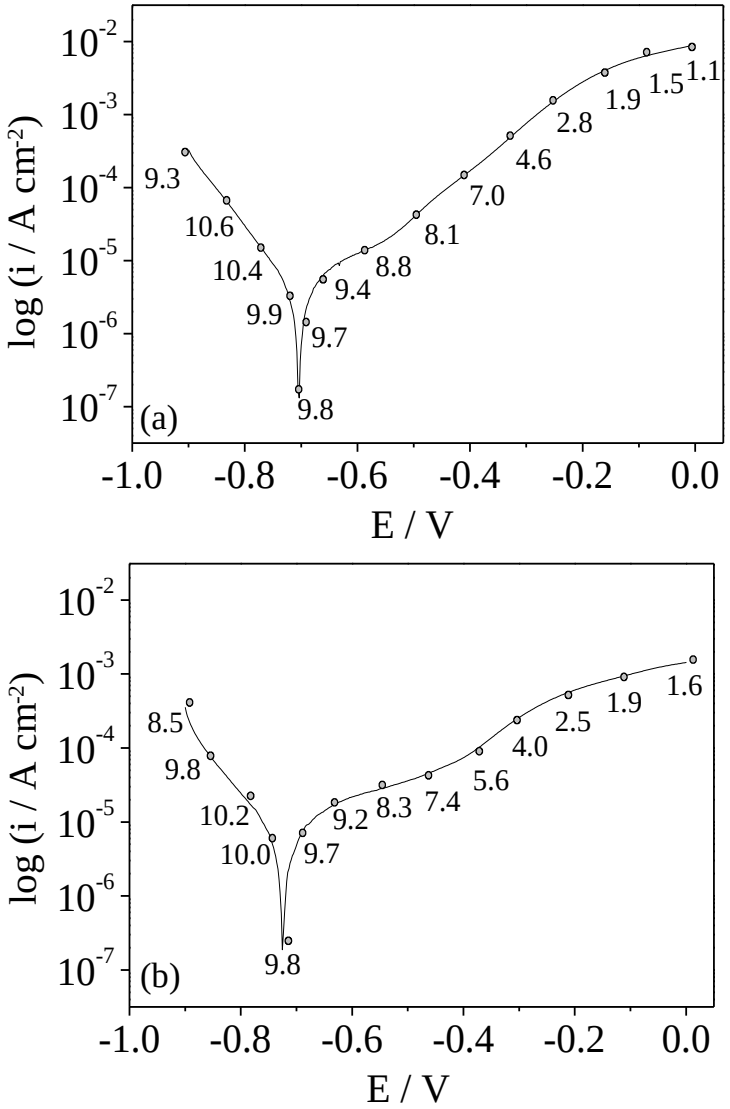

Figure 6. Potentiodynamic polarization curves and local pH obtained in 0.1 mol dm^{-3} NaCl solution at 1 mV s^{-1} for the Ni-4W and Ni-15Mo-4W coatings obtained at 60 mA cm^{-2}.

The local pH of the cathodic branch is alkaline. This behaviour was related with the oxygen reduction that was the cathodic reaction in 0.1 mol dm^{-3} NaCl solution (reaction 1). In the anodic branches of the Figures 6a and 6b, the pH was 9.8 at the corrosion potential and changed to acid values in function of the applied potential became more positive.

$$H_2O_{(l)} + \frac{1}{2}O_{2(g)} + 2e^- \rightarrow 2OH^-_{(aq)} \quad (1)$$

According to Pourbaix diagrams [19], the nickel oxidizes to $Ni(OH)_2$ in the interval between 6 and 12 and that the Ni^{2+} specie is stable only at acid pH. The reactions associated with the Ni oxidation are shown below.

$$Ni_{(s)} + 2H_2O_{(l)} \rightarrow Ni(OH)_{2(s)} + 2H^+_{(aq)} + 2e^- \quad (2)$$

$$Ni_{(s)} \rightarrow Ni^{2+}_{(aq)} + 2e^- \quad (3)$$

Li-yuan *et al.* [20] studied the effect of grain size on corrosion behavior of electrodeposited Ni in acidic, neutral and alkaline medium. The authors showed that the Ni layers presented an active-passive behavior in the alkaline and neutral solutions, while in acid solutions the Ni layer corrodes. The authors confirmed the presence of $Ni(OH)_2$ and NiO in the passive films by XPS surface analysis. Therefore, the pH variation between 9.8 and 6.0 observed in the anodic branch of the polarization curve was associated to the oxidation of Ni to $Ni(OH)_2$.

The tungsten's potential-pH diagram [19] showed that in alkaline and acidic media the oxidation of W to WO_4^{2-} ion and to WO_2 are preferred, respectively, and that the oxidation of WO_2 to WO_3 occurs at high potential and in acidic medium. Therefore, the following reactions are considered:

$$W_{(s)} + 4H_2O_{(l)} \rightarrow WO^{2-}_{4(aq)} + 8H^+_{(aq)} + 6e^- \quad (4)$$

$$W_{(s)} + 2H_2O_{(l)} \rightarrow WO_{2(s)} + 4H^+_{(aq)} + 4e^- \quad (5)$$

$$WO_{2(s)} + H_2O_{(l)} \rightarrow WO_{3(s)} + 2H^+_{(aq)} + 2e^- \quad (6)$$

$$WO_{2(s)} + 2H_2O_{(l)} \rightarrow WO^{2-}_{4(aq)} + 4H^+_{(aq)} + 2e^- \quad (7)$$

Anik e*t al.* [21] claim that the stability of oxide film on W was greater in acidic and weakly alkaline solutions, since tungsten oxide film on W surface suffers dissolution in alkaline medium forming tungstate ion. Therefore, the presence of the unstable WO_2 that dissolve as WO_4^{2-} (reaction 7) was proposed since the values of the local pH were alkaline between –0.7 V and –0.4 V and higher slope of the potential – current density curve observed for the Ni-4W coating in this potential range (Fig. 5 and 6a).

For applied potentials more positive than –0.4 V, the acid pH values were observed in indicating that the current values can be associated to the Ni dissolution.

The oxidation of molybdenum to $MoO_{2(s)}$ was preferred in the interval of pH 3 to pH 10. At high potential and acidic medium, MoO_2 is oxidizes to MoO_3. Molybdate ion was the specie that it was present in neutral and alkaline solution, while at high potential and weakly acidic solutions there was the formation of $HMoO_4^-$ [19]. The reactions described above are shown below:

$$Mo_{(s)} + 2H_2O_{(l)} \rightarrow MoO_{2(s)} + 4H^+_{(aq)} + 4e^- \quad (8)$$

$$MoO_{2(s)} + H_2O_{(l)} \rightarrow MoO_{3(s)} + 2H^+_{(aq)} + 2e^- \quad (9)$$

$$MoO_{2(s)} + 2H_2O_{(l)} \rightarrow MoO^{2-}_{4(aq)} + 4H^+_{(aq)} + 2e^- \quad (10)$$

$$MoO_{2(s)} + 2H_2O_{(l)} \rightarrow HMoO^{2-}_{4(aq)} + 3H^+_{(aq)} + e^- \quad (11)$$

Badawy and Al-Kharafi [22] analyzed corrosion and passivation behaviours of molybdenum in aqueous solution at different pH. They proposed that in acidic solutions the passive film consisted mainly of MoO_2 and MoO_3. The authors showed that the oxide film on Mo was relatively more stable in acidic solutions compared to the neutral and alkaline solutions.

As shown in the polarization curve of the Ni-Mo-W coating (Fig. 6), the local pH was alkaline between –0.7 and –0.4, suggesting the formation of the WO_2 and MoO_2 that can dissolve as WO_4^{2-} and MoO_4^{2-} according to the reactions 7 and 10.

Thus, the decrease of the local pH in the acid direction observed in the polarization curves of the binary and ternaries coatings was attributed to the formation of $Ni(OH)_2$ (reaction 2) and the dissolution of WO_2 and MoO_2 to WO_4^{2-} (reaction 7) MoO_4^{2-} (reaction 10) species.

The corrosion of Ni-4W, Ni-15Mo-4W and Ni-21Mo-5W coatings obtained was also evaluated over the course of 480 minutes in 0.1 mol dm^{-3} NaCl electrolyte at open circuit potential (E_{oc}) and the results are displayed in Figure 7. For all coatings, the E_{oc} values became nobler with time indicating the formation of a film on the coating surface such as metal oxides and metal hydroxides, which kinetically limit the dissolution of the coatings at E_{oc}. In NaCl medium, the E_{oc} values were not influenced by the composition of the ternary coating. However, Ni-4W coatings showed slightly higher E_{oc} at the end of the test, which was attributed to higher Ni content, leading to a higher superficial concentration of $Ni(OH)_2$ on the coating surface when compared with ternary coatings.

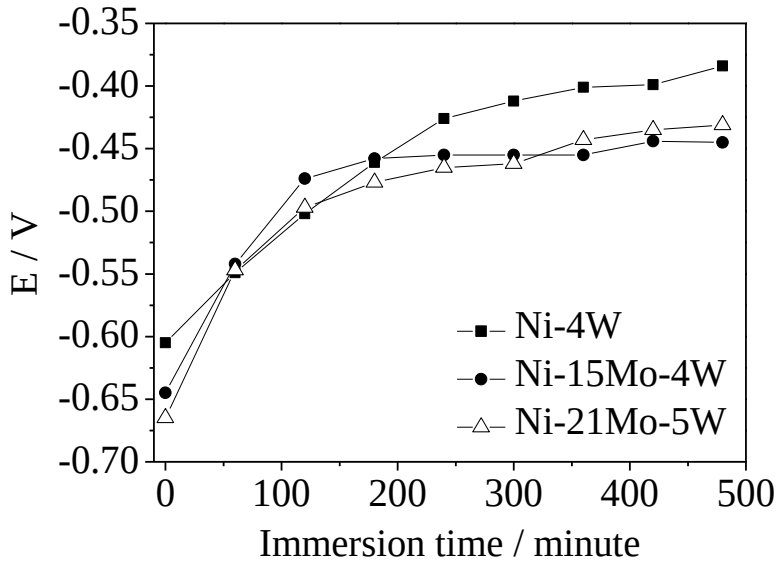

Figure 7. Variation of the open circuit potential with immersion time in 0.1 mol dm^{-3} NaCl solution for the electrodeposited Ni-4W, Ni-15Mo-4W and Ni-21Mo-5W coatings.

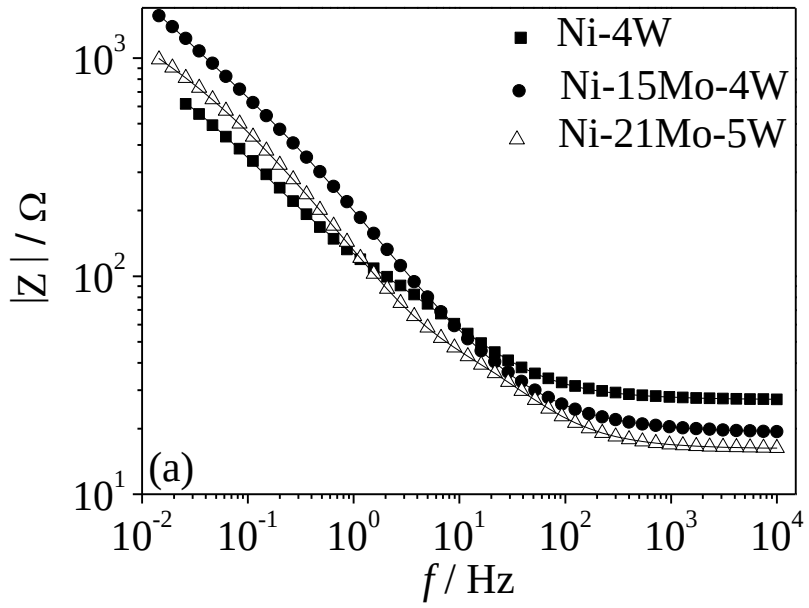

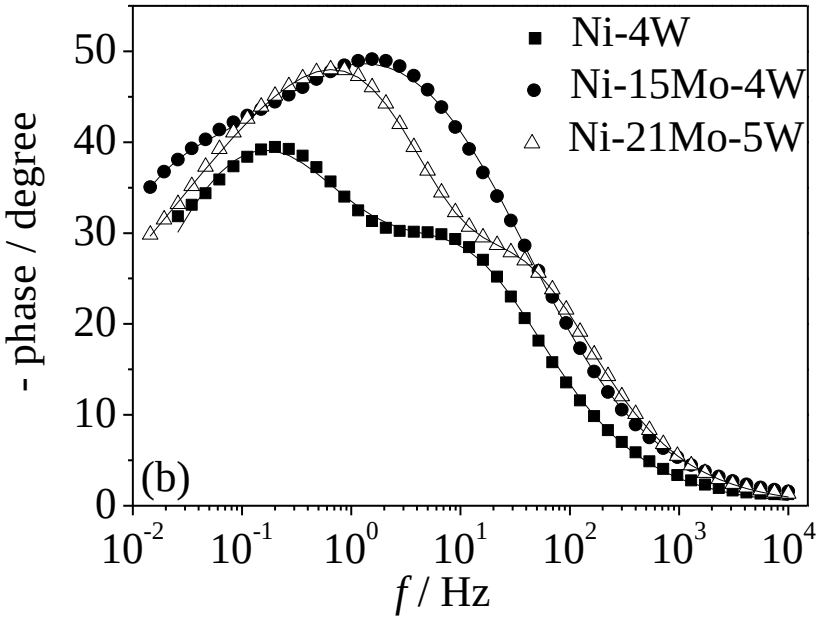

Figure 8. Experimental impedance spectra (symbols) obtained at E_{oc} for Ni-4W, Ni-15Mo-4W and Ni-21Mo-5W coatings immersed in 0.1 mol dm^{-3} NaCl for 480 min. The continuous lines are the spectra simulated using the equivalent electric circuits.

The influence of the immersion time on corrosion behavior of the studied samples was also evaluated by electrochemical impedance spectroscopy. Figure 8 presents the evolution of the impedance spectra obtained at E_{oc} for Ni-4W, Ni-15Mo-4W and Ni-21Mo-5W coatings for 480 min of immersion in 0.1 mol dm^{-3} NaCl aqueous solution.

The spectra obtained in 0.1 mol dm^{-3} NaCl medium presented two time constants for Ni-4W and Ni-15Mo-4W coatings and three time constants for Ni-21Mo-5W coating (Figures 8). For the Bode diagrams that show two time constants, first the time constant observed at higher frequency range was explained as due to the hydroxide or oxide films responses related to the presence of $Ni(OH)_2$, WO_2 and MoO_2 on the coating surface. The second time constant observed at low frequency range was attributed to charge transfer process for coatings reacting with NaCl solution [23, 24].

For the Bode diagrams that exhibited three time constants, the first time constant, observed at high frequency range, was related to the formation of a secondary oxide layer formed over the primary oxide layer formed [25]. The second time constant, observed at medium frequency range, was attributed to the response of the primary oxide film formed on the coating surface. The third time constant located at low frequency range was related to charge transfer process for coatings reacting with NaCl solution.

The linear relationship between log $|Z|$ and log f was observed for all coatings (Figs 8a), but with different slopes less than –1 and phase angle maxima less than 90^o. According to Metikoš-Huković *et al.* [26, 27], these results indicated that the hydroxides and oxides films formed on the coating surface at open circuit potentials were not fully capacitive. In order to fit and analyze the impedance data, two and three time constants electrochemical equivalent circuits were used (Fig. 9). Since the measured capacitive response was not generally ideal due to the certain heterogeneity and

roughness of the coating surface, a constant phase element (CPE) was introduced for fitting the spectra [27-29]. The impedance values can be described by empirical function $Z(CPE)=[Q(j\omega)^n]^{-1}$, where the constant Q account for a combination of properties related to both the surface and the electroactive species, $j\omega$ is the complex variable for sinusoidal perturbations, and n being the exponent of CPE, with values between –1 and 1 [30]. The adjustment between the fitted and the experimental diagrams are shown in the Figure 8.

In the selected equivalent circuit for two time constants, R_s corresponds to the electrolyte resistance; R_1 and CPE_1 are the charge transfer resistance at hydroxide-oxide film/electrolyte interface and non-ideal double layer capacitance, respectively. R_2 and CPE_2 are the coating resistance and the coating capacitance. In the selected equivalent circuit for three time constants, R_s corresponds to the electrolyte resistance; R_1 and CPE_1 is the charge transfer resistance at secondary hydroxide-oxide film/electrolyte interface and non-ideal double layer capacitance, respectively. R_2 and CPE_2 is the resistance at primary hydroxide-oxide film and capacitance of the hydroxide-oxide film, respectively. R_3 and CPE_3 is the resistance at coating and the coating capacitance, respectively. The values of circuit´s element for the studied coating are listed in Table 1 and 2.

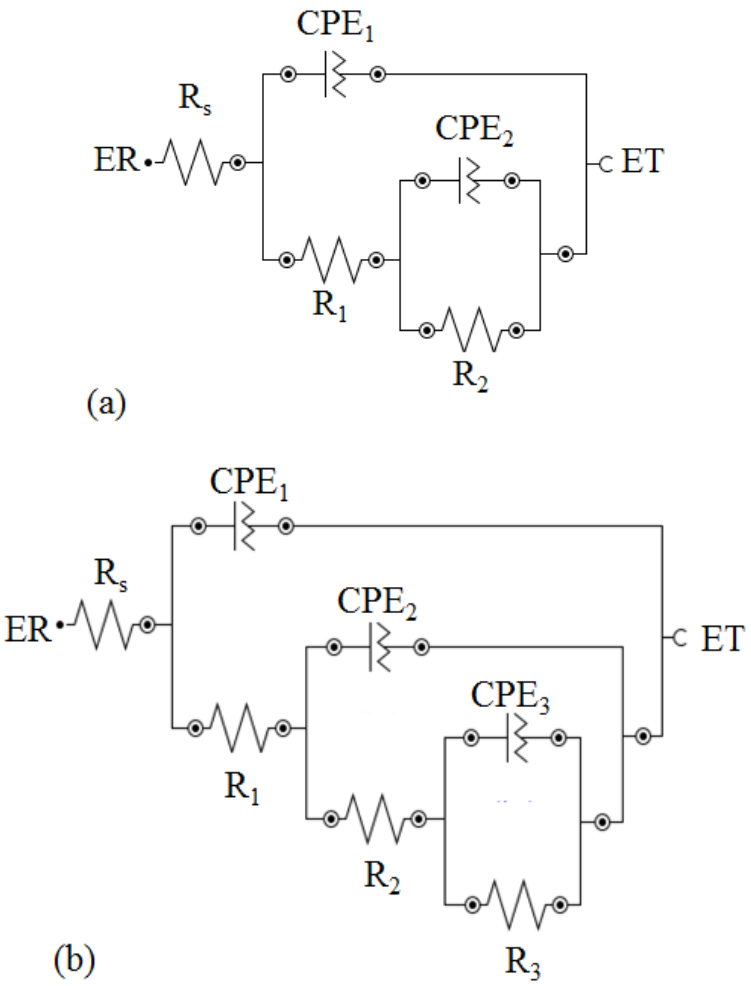

Figure 9. Equivalent circuit representing the corrosion of coatings in 0.1 mol dm^{-3} NaCl solution.

The factor *n* is adjustable parameters that usually lie between 0.5 and 1. When *n* = 1, the CPE describes an ideal capacitor and when *n* = 0.5 the CPE represents a Warburg impedance with diffusional character [26, 29]. The values of the factor *n* obtained by fitting the impedance data this work were between 0.43 and 0.77 for all studied samples. According to Hamadou *et al.*, [25] this variation was associated to the heterogeneity and complexity of electrode surface.

Table 1. Fitting results for the impedance spectra obtained after immersion time of 480 min in 0.1 mol dm^{-3} NaCl for the impedance spectra with two time constants [R(Q[R(QR)])].

Ni-4W coating						
R_s (Ω)	$10^5 \times Q_1$ ($\Omega^{-1} s^n$)	n_1	R_1 (Ω)	$10^4 \times Q_2$ ($\Omega^{-1} s^n$)	n_2	R_2 (Ω)
27.2	162	0.73	97	31.6	0.67	1014
Ni-15Mo-4W coating						
R_s (Ω)	$10^5 \times Q_1$ ($\Omega^{-1} s^n$)	n_1	R_1 (Ω)	$10^4 \times Q_2$ ($\Omega^{-1} s^n$)	n_2	R_2 (Ω)
19.2	144	0.66	1293	24.2	0.71	2497

Table 2. Fitting results for the impedance spectra obtained after immersion time of 480 min in 0.1 mol dm^{-3} NaCl for the impedance spectra with three time constants [R(Q[R(Q[R(QR)])])].

Ni-21Mo-5W coating									
R_s (Ω)	$10^5 \times Q_1$ ($\Omega^{-1} s^n$)	n_1	R_1 (Ω)	$10^5 \times Q_2$ ($\Omega^{-1} s^n$)	n_2	R_2 (Ω)	$10^5 \times Q_3$ ($\Omega^{-1} s^n$)	n_3	R_3 (Ω)
16.2	68	0.77	49.3	69.7	0.95	47.4	182	0.43	2670

The coating resistances values and hydroxide-oxides resistances values increased with the presence of molybdenum. This result was in agreement with the data from the open circuit potential. It was observed high value in the constants *Q* in low frequencies for coatings with same number of time constant and lower content of Mo. Özkan *et al.* [23] and Bekish *et al.* [28] reported that the observance of a higher capacitance CPE for coating can be ascribed to the more contact area of coating and electrolyte as well as the access of electrolyte into the pores of the coating or may be attributed to formation of a film less compact. The decrease of constants *Q* indicated the smoother and protective nature of passive film formed on coatings [20, 23].

4. CONCLUSION

Ni-W and Ni-Mo-W coatings were successfully obtained by electrodeposition using direct current and the Mo content in the layer increase with the molybdenum ion concentration in the electrolyte. Cracked and non-cracked coatings were obtained and the electrodeposited coatings were

nanocrystalline or amorphous. The experimental thickness was influenced slightly by the MoO_4^{2-} concentration in the plating solution. The decreases in the coating thickness was observed with increase of MoO_4^{2-} concentration. For applied potential more positive potential than –0.55 V, anodic current densities of the potentiodynamic polarization curves, of the ternary alloys, were lower than anodic current density of the binary alloy showing that the addition of Mo improved the corrosion resistance of the Ni-W based coatings in neutral. The formation of surface films oxides and hydroxides, that can blocked the dissolution of coatings, was elucidated with local pH measurements. The local pH values showed favorable formation theses oxides e hidroxides as corrosion product. The results of fit of the electrochemical impedance spectra in the ternary coatings corroborate to formation of a secondary oxide layer formed over the primary oxide layer formed.

ACKNOWLEDMENTS

The authors gratefully acknowledge the CNPq (Edital Universal/CNPq 14/2013 project 470960/2013-2), CAPES, FINEP and FUNCAP (Brazil) for financial assistance. The authors acknowledge the use of SEM facilities from IPDI and the use of diffractometer facilities from LRX-UFC.

References

1. G. Saravanan and S. Mohan, *Corros. Sci.* 51 (2009) 197-202.
2. W-Y Chen, S-K Tien, F-B Wu and J-G Duh, *Surf. Coat. Tech.* 182 (2004) 85-91.
3. P. Lima-Neto, A. N. Correia, R. A. C. Santana, R. P. Colares, E. B. Barros, P. N. S. Casciano and G. L. Vaz, *Electrochim. Acta* 55 (2010) 2078-2086.
4. J. Emsley, *The Elements*, third ed., Oxford, England, 1998.
5. S. Yari and C. Dehghanian, *Ceram. Int.* 39 (2013) 7759-7766.
6. E. Goméz, E. Pellicer and E. Vallés, *J. Electroanal. Chem.* 556 (2003) 137-145.
7. E. Goméz, E. Pellicer and E. Vallés, *Surf. Coat. Tech.* 197 (2005) 238-246.
8. O. Younes and E. Gileadi, *J. Electroanal. Chem.* 149 (2002) 100-111.
9. H. Alimadadi, M. Ahmadi, M. Aliofkhazraei and S. R. Younesi, *Mater. Design.* 30 (2009) 1356-1361.
10. S. Z. E. Abedin, *J. Appl. Electrochem.* 31 (2009) 711-718.
11. C. G. Silva, I. C. P. Margarit-Mattos, O. R. Mattos, H. Perrot, B. Tribollet and V. Vivier, *Corros. Sci.* 51 (2009) 151-158.
12. J. A. Calderón, O. R. Matos, O. E. Barcia, S. I, C. Torresi and J. E. P. Silva, *Electrochim. Acta* 47 (2002) 4531-4541.
13. S. Sun and E. J. Podlaha, *J. Electrochem. Soc.* 159 (2012) 97-102.
14. P. Lammel, L. D. Rafailovic, M. Kolb, K. Pohl, A. H. Whitehead, G. Grundmeier and B. Gollas, *Surf. Coat. Tech.* 206 (2012) 2545-2551.
15. N. Eliaz, T. M. Sridhar and E. Gileadi, *Electrochim. Acta* 50 (2005) 2893-2904.
16. I. Mizushima, P. T. Tang, H. N. Hansen and M. A. J. Somers, *Electrochim. Acta* 51 (2006) 6128-6134.
17. H. Wang, R. Liu, F. Cheng, Y. Cao, G. Ding and X. Zhao, *Microelectron. Eng.* 87 (2010) 1901-1906.
18. I. Mizushima, P.T. Tang, H. M. Hansen and M. A. J. Somers, *Electrochim. Acta* 51 (2005) 888-896.
19. M. Pourbaix, *Atlas of Electrochemical Equilibria in Aqueous Solutions*, New York, USA, 1966.
20. Q. Li-yuan, L. Jian-she and J. Qing, *Trans. Nonferrous Met. Soc. China* 20 (2010) 82-89.
21. M. Anik, T. Cansizoğlu and S. Çevik, *Turk. J. Chem.* 28 (2004) 425-439.

22. W. A. Badaway and F. M. Al-kharafi, *Electrochim. Acta* 44 (1998) 693-702.
23. S. Özkan, G. Hapçi, G. Orhan and K. Karmanli, *Surf. Coat. Tech.* 232 (2013) 734-741.
24. K. Krishnaveni, T. S. N. Sankara Narayanan and S. K. Seshadri, *J. Alloys Compd.* 480 (2009) 765-770.
25. L. Hamadou, A. Kadri and N. Benbrahim, *Appl. Surf. Sci.* 252 (2005) 1510-1519.
26. M. Metikoš-Huković and R. Babić, *Corros. Sci.* 49 (2007) 3570-3579.
27. M. Metikoš-Huković, Z. Pilić, R. Babić and D. Omanović, *Acta Biomater.* 2 (2006) 693-700.
28. Y. N. Bekish, S. K. Poznyak, L. S. Tsybulskaya and T. V. Gaevskaya, *Electrochim. Acta* 55 (2010) 2223-2231.
29. A.M. E. Orazem and B. Tribollet, *Electrochemical Impedance Spectroscopy*, New Jersey, USA, 2008.
30. S. Tamilselvi, V. Raman and N. Rajendran, *Electrochim. Acta* 52 (2006) 839-846.